

Luminescent Carbazole-Based Eu^{III} and Yb^{III} Complexes with a High Two-Photon Absorption Cross-Section Enable Viscosity Sensing in the Visible and Near IR with One- and Two-Photon Excitation

Jorge H. S. K. Monteiro, Natalie R. Fetto, Matthew J. Tucker, and Ana de Bettencourt-Dias*



Cite This: *Inorg. Chem.* 2020, 59, 3193–3199



Read Online

ACCESS |



Metrics & More

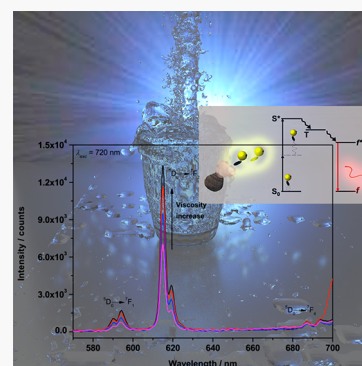


Article Recommendations



Supporting Information

ABSTRACT: The newly synthesized Eu^{III} and Yb^{III} complexes with the new carbazole-based ligands CPAD²⁻ and CPAD⁴⁻ display the characteristic long-lived metal-centered emission upon one- and two-photon excitation. The Eu^{III} complexes show the expected narrow emission bands in the red region, with emission lifetimes between 0.382 and 1.464 ms and quantum yields between 2.7% and 35.8%, while the Yb^{III} complexes show the expected emission in the NIR region, with emission lifetimes between 0.52 and 37.86 μ s and quantum yields between 0.028% and 1.12%. Two-photon absorption cross sections (σ_{2PA}) as high as 857 GM were measured for the two ligands. The complexes showed a strong dependence of the one- and two-photon sensitized emission intensity on solvent viscosity in the range of 0.5–200 cP in the visible and NIR region.



INTRODUCTION

Lanthanide (Ln^{III}) ions are interesting as luminescent labels and sensors for a variety of applications.^{1–15} The luminescence is color pure, due to the core nature of the *f* orbitals involved in the emission, and is long-lived, due to the forbidden nature of the *f*–*f* transitions, which enables time-delayed emission spectroscopy with increased signal-to-noise ratio.^{16–18} The forbidden transitions render direct excitation inefficient, and thus the emission is sensitized through an appended ligand chromophore (Figure 1). This is referred to as the antenna effect and leads to a large Stokes shift of sensitized emission, which is advantageous due to separation of excitation and emission wavelengths. In addition, ligands are easily derivatized, which enables tuning the chemical and spectroscopic properties of the complexes. Typically, chromophores absorb in the high-energy region of the spectrum,^{19,20} and these wavelengths have low tissue penetration and result in radiation damage, thus making them undesirable for bioimaging applications.^{21–24} Excitation at lower nondamaging energies is achieved using ligands with extended aromatic systems that absorb in the visible; however, the low energy singlet (S) and triplet (T) states cannot sensitize visible emitting Ln^{III} ions.^{16,25} An alternative is to use two-photon absorption (2PA),^{21,22,26–29} a nonlinear process where two photons with half the energy required by the one-photon excitation (1PA) are absorbed simultaneously (Figure 1).^{30,31} Organic dyes³² and transition-metal complexes³³ can be efficient photoluminescent labels for 2PA imaging, but they are often affected by photobleaching and have short emission lifetimes and narrow Stokes shifts, which limit their usefulness. Nano-

particles also have been frequently studied for this purpose, although their synthesis and purification are not always straightforward and they might suffer from solubility issues.³⁴ Ln^{III} ion complexes do not suffer from these limitations, as indicated above, and are therefore great candidates for 2PA imaging.

Lakowicz and co-workers pioneered the sensitization of Eu^{III} emission using 2PA.^{35,36} Since then, the use of luminescent Ln^{III} complexes as 2PA labels and sensors has flourished, and examples of both visible and NIR emitters are known.^{37–49} Andraud, Maury, and co-workers studied 2PA-sensitization of Eu^{III} complexes with dipicolinato- and cyclononane-based ligands and concluded that ligands with charge-transfer (CT) states have improved 2PA cross sections (σ_{2PA}).^{49–51}

Physicochemical properties of biological systems provide important information regarding physiological processes. For example, viscosity plays an important role in the intra- and extracellular mass transport,^{52,53} and abnormalities in blood and plasma viscosity are indicative of diabetes and hypertension.^{52,54,55} Viscosity of macroscopic systems is easily determined, yet the same methods cannot be applied at cellular level.⁵² Organic dyes, such as molecular rotors, have been used as luminescent viscosity sensors.^{56–58} To date, only one Ln^{III}-based viscosity sensor has been reported, by Zhang

Received: December 6, 2019

Published: February 13, 2020

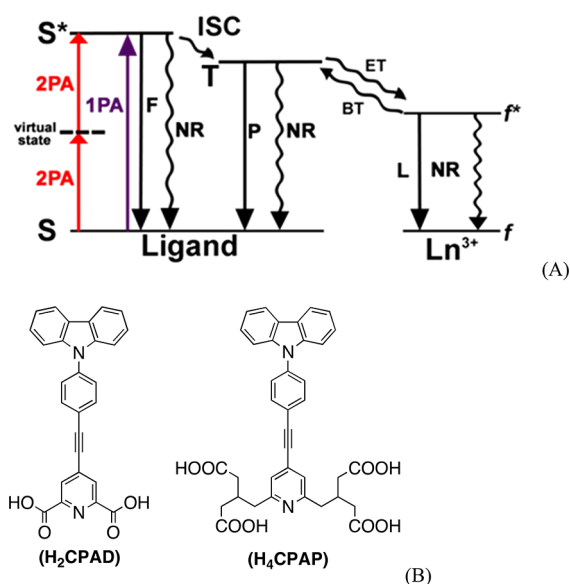


Figure 1. (A) Energy level diagram illustrating the antenna effect for Ln^{III} . 2PA and 1PA, the two- and one-photon absorption, respectively; F, fluorescence; P, phosphorescence; ISC, intersystem crossing; ET, energy transfer; BT, back transfer; L, luminescence; NR, nonradiative pathways; S and T, states with singlet and with triplet multiplicity, respectively. (B) Molecules studied in this work.

and co-workers. Their Yb^{III} porphyrinato complexes with a Kläui ligand displayed emission lifetimes τ that varied by a factor of ~ 2.8 in the viscosity range of 0.52–1200 cP.⁵⁹ Since viscosity alters the population of intramolecular charge transfer states, molecules with such states should provide a unique opportunity to sense it.⁶⁰

De Bettencourt-Dias and co-workers reported a carbazole-substituted dipicolinato as sensitizer of Eu^{III} and Tb^{III} emission.^{61,62} Carbazole is known for its 2PA properties.^{63–65} Thus, with the goal of increasing our knowledge of 2PA-sensitized Ln^{III} emission and expanding the availability of Ln^{III} -based viscosity sensors, we isolated two new carbazole-based ligands with potential CT states,^{50,62} CPAD²⁻ (4-((4-(9H-carbazol-9-yl)phenyl)ethynyl)pyridine-2,6-dicarboxylate) and CPAP⁴⁻ (2,2'-(4-((4-(9H-carbazol-9-yl)phenyl)(pyridine-2,6-diyl)bis(methylene)dimalonate) and their Ln^{III} complexes ($\text{Ln}^{\text{III}} = \text{Eu}^{\text{III}}, \text{Gd}^{\text{III}}, \text{and Yb}^{\text{III}}$).

RESULTS AND DISCUSSION

Synthesis and Characterization of the H_2CPAD and H_4CPAP Ligands and of the Ln^{III} Complexes. H_2CPAD and H_4CPAP (Figure 2A) were synthesized through modified literature procedures (Scheme S1) and characterized using standard techniques (Figures S2, S4, S6, S8, S10, and S12). The Ln^{III} ($\text{Ln}^{\text{III}} = \text{Eu}^{\text{III}}, \text{Gd}^{\text{III}}, \text{Yb}^{\text{III}}$) complexes were obtained as yellow solids in $\sim 70\%$ yield by reacting LnCl_3 with K_2CPAD in a 1:3 metal-to-ligand ratio and with K_4CPAP in a 1:1 metal-to-ligand ratio in water/DMF (1:20). They were characterized by mass spectrometry (Figures S13–S18) and shown to be photostable (Figure S19).

One-Photon Spectroscopy Studies of the $\text{K}_3[\text{Ln}(\text{CPAD})_3]$ and $\text{K}[\text{Ln}(\text{CPAP})(\text{L})_2]$ ($\text{Ln} = \text{Eu}^{\text{III}}$ or Yb^{III} and $\text{L} = \text{DMSO}$ or H_2O) Complexes. $\text{K}_3[\text{Ln}(\text{CPAD})_3]$ and $\text{K}[\text{Ln}(\text{CPAP})(\text{L})_2]$ ($\text{Ln} = \text{Eu}^{\text{III}}$ or Yb^{III} and $\text{L} = \text{DMSO}$ or H_2O) in solution display the characteristic Eu^{III} -centered $^5\text{D}_0 \rightarrow ^7\text{F}_j$ ($j = 0–4$) (Figure 2A, right) and Yb^{III} -centered $^2\text{F}_{5/2} \rightarrow$

$^2\text{F}_{7/2}$ transitions in the emission spectra (Figure 3, right). Different splitting patterns in the emission spectra are a result of different coordination environments around the metal ion, due to the different ligand binding.¹⁷ The excitation spectra (Figures 2B and 3 left) closely resemble the absorption spectra of the ligands (Figure S22), indicating that the ligands sensitize the metal-centered emission.

The excited state lifetimes (τ) and emission efficiencies ($\Phi_{\text{L}}^{\text{Eu}}$) of the complexes are summarized in Table 1. The τ values of 1.464 ms for $[\text{Eu}(\text{CPAD})_3]^{3-}$ and 1.702 ms for $[\text{Eu}(\text{CPAP})(\text{DMSO})_2]^-$ were measured in DMSO. In water/DMSO (9:1), the latter complex shows an emission lifetime of 382 μs , consistent with exchange of the coordinated DMSO molecules for water (vide infra). The long excited state lifetimes are accompanied by high intrinsic quantum yields ($\Phi_{\text{Eu}}^{\text{Eu}}$) in DMSO and a lower value for the complex in water. $\Phi_{\text{L}}^{\text{Eu}}$ values of 31.7%, 35.8%, and 2.7% were observed for $[\text{Eu}(\text{CPAD})_3]^{3-}$, $[\text{Eu}(\text{CPAP})(\text{DMSO})_2]^-$, and $[\text{Eu}(\text{CPAP})(\text{H}_2\text{O})_2]^-$, respectively. Compared with $\text{Cs}_3[\text{Eu}(\text{dpa})_3]$ (dpa = dipicolinato) in DMSO (Table S1), the lower emission efficiencies are consistent with an increase in the donor–acceptor distances R_{L} (Table 1)⁶¹ and quenching caused by O–H vibrational coupling in the case of $[\text{Eu}(\text{CPAP})(\text{H}_2\text{O})_2]^-$ (vide infra). The favorable energies of S and T states of the ligands result in high η_{sens} for the Eu^{III} complexes (Table 1). $\Phi_{\text{L}}^{\text{Yb}}$ values of 0.75% and 0.028% were observed for $[\text{Yb}(\text{CPAP})(\text{DMSO})_2]^-$ and $[\text{Yb}(\text{CPAP})(\text{H}_2\text{O})_2]^-$, respectively (Table 1). These values are similar to related dipicolinato-based complexes and compare favorably with known compounds.^{45,47,48,67,68} The emission lifetimes for the $[\text{Yb}(\text{CPAP})(\text{L})_2]^-$ complex ($\text{L} = \text{H}_2\text{O}$ or DMSO) show a similar behavior. The τ is longer for $\text{L} = \text{DMSO}$ at 8.91 μs than for $\text{L} = \text{H}_2\text{O}$ at 0.52 μs , as is to be expected due to quenching through the O–H oscillators.

In the case of the Ln^{III} complexes with the ligand CPAP⁴⁻, a decrease in the emission efficiency and lower τ in TRIS/HCl buffered aqueous system (pH ~ 7.4 , 10% DMSO), compared with the DMSO solution, are observed. This decrease is a result of the nonradiative deactivation of the Ln^{III} excited state by the O–H vibrations of coordinated water molecules. The presence of two coordinated water molecules q was confirmed for the Eu^{III} complex by comparing τ in water ($\tau_{\text{H}_2\text{O}}$) and D_2O ($\tau_{\text{D}_2\text{O}}$) (eq S5 and Table 1).

Two-Photon Spectroscopy Studies of the $\text{K}_3[\text{Ln}(\text{CPAD})_3]$ and $\text{K}[\text{Ln}(\text{CPAP})(\text{L})_2]$ ($\text{Ln} = \text{Eu}^{\text{III}}$ or Yb^{III} and $\text{L} = \text{DMSO}$ or H_2O) Complexes. All Eu^{III} complexes can be excited with a wide range of low energy photons in a 2PA process (Figure S32). By exciting at 720 or 750 nm, with the latter chosen for comparison with the 2PA standard rhodamine B,⁶⁹ the characteristic metal-centered emission pattern is observed (Figures 2B and S29a–S31a). The quadratic dependence of the emission intensity I on the laser power P (Figures 2C and S29b–S31b, Tables 2 and S2) confirmed the 2PA process. The emission spectra obtained by one- or two-photon excitation are the same (Figures 2 and S29–S31), indicating that the same excited states are involved in the process.

The two-photon absorption cross sections ($\sigma_{2\text{PA}}$) are summarized in Table 2. A value of 857 GM was obtained for $\text{K}_3[\text{Eu}(\text{CPAD})_3]$. This is among the highest reported for Eu^{III} complexes in solution, such as 775 GM for $[\text{NBu}_4]_3[\text{Eu}(\text{dpaS})_3]$ described by Maury, Andraud, and co-workers.⁴⁵

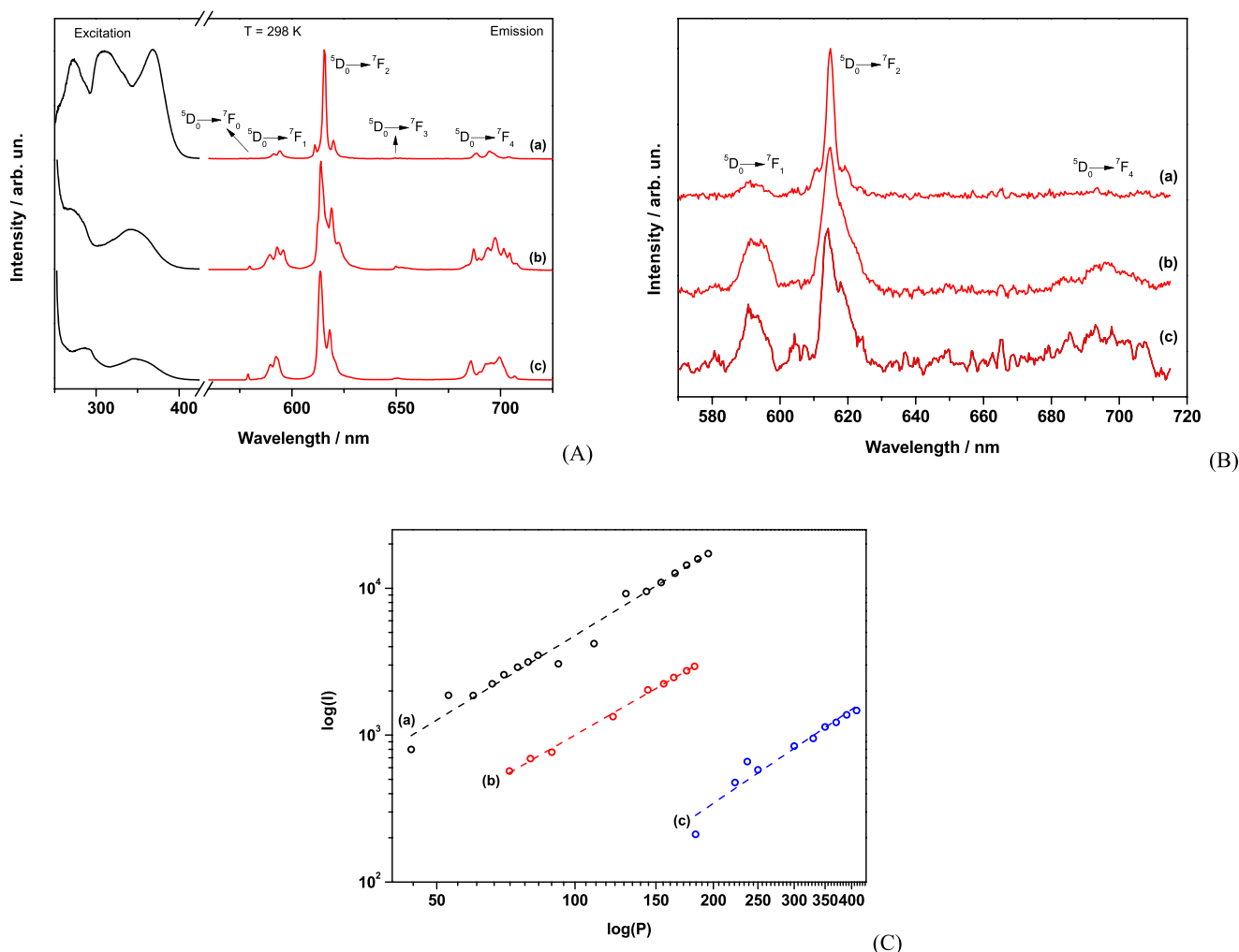


Figure 2. (A) 1PA excitation (black lines, left) and emission spectra (red lines, right) of Eu^{III} complexes ($\lambda_{\text{exc}} = 380$ nm). (B) 2PA emission spectra of Eu^{III} complexes. (C) Plot of the log of the emission intensity I at 615 nm upon 2PA excitation as a function of the log of the laser power P . From top to bottom in each figure: (a) K₃[Eu(CPAD)₃] in DMSO, (b) K[Eu(CPAP)(DMSO)₂] in DMSO, and (c) K[Eu(CPAP)(H₂O)₂] in TRIS/HCl buffered aqueous system (pH \sim 7.4, 10% DMSO); $\lambda_{\text{exc}} = 720$ nm; [complex] = 1×10^{-4} M.

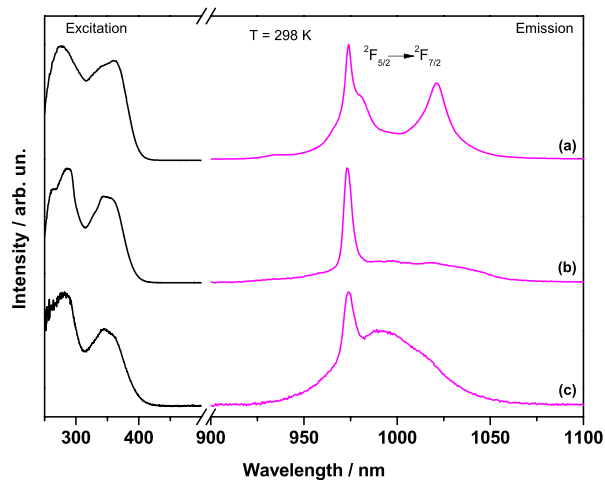


Figure 3. Excitation (black lines, left) and emission spectra (pink lines, right) of Yb^{III} complexes: (a) K₃[Yb(CPAD)₃] in DMSO ($\lambda_{\text{exc}} = 370$ nm), (b) K[Yb(CPAP)(DMSO)₂] in DMSO ($\lambda_{\text{exc}} = 350$ nm), and (c) K[Yb(CPAP)(H₂O)₂] in TRIS/HCl buffered aqueous system (pH \sim 7.4, 10% DMSO) ($\lambda_{\text{exc}} = 350$ nm) [complex] = 1×10^{-4} M.

Sensitization of Eu^{III} using 2PA is not commonly reported for complexes with coordinated solvent molecules because the latter often quench the emission. Parker and co-workers found a $\sigma_{2\text{PA}}$ of 1.7 and 0.4 GM for aqueous solutions of [Eu(do2ax1)(H₂O)](OTf)₃ and [Eu(do2ax2)(H₂O)](OTf)₃, respectively (do2ax1 and do2ax2 are dota derivatives with appended *SH*-thiocromeno[2,3-*b*]pyridine-5-one and methyl 5-oxo-*SH*-thiocromeno[2,3-*b*]pyridine-7-carboxylate, respectively).⁴³ We were pleasantly surprised to determine a $\sigma_{2\text{PA}}$ of 228 GM for the K[Eu(CPAP)(H₂O)₂] in TRIS/HCl buffered aqueous system (pH \sim 7.4, 10% DMSO), similar to the value in DMSO, consistent with the fact that $\sigma_{2\text{PA}}$ is intrinsic to the ligand and not affected by the solvent.⁷⁰ This value also indicates that CPAP⁴⁻, which yields complexes soluble in water/DMSO, is viable for 2PA bioimaging, although this application is not shown here.

Viscosity-Sensing Studies using the K₃[Ln(CPAD)₃] (Ln = Eu^{III} or Yb^{III}) Complexes. The temperature-dependent phosphorescence spectra of K₃[Gd(CPAD)₃], with maxima at 510 nm at 298 K and 435 nm at 77 K (Figure S33), indicate that a twisted intramolecular charge-transfer (TICT) state is present in CPAD²⁻, involving the carbazole and phenyl rings.^{62,71} As mentioned above, changes in the viscosity often

Table 1. Singlet (S) and Triplet (T) State Energies of the Ligands, Lifetime (τ), Intrinsic Emission Efficiency (Φ_{Ln}^{Ln}), Quantum Yield (Φ_L^{Ln}) of Sensitized Efficiency, Sensitization Efficiency (η_{sens}), and the Number of Coordinated Water Molecules (q) for the Complexes at $\lambda_{exc} = 360$ nm

complex	solvent	S ^a [cm ⁻¹]	T ^a [cm ⁻¹]	τ	Φ_{Ln}^{Ln} [%]	Φ_L^{Ln} [%]	η_{sens} [%]	R _L [Å]	q
K ₃ [Eu(CPAD) ₃]	DMSO	23520 ± 460	19690 ± 300	1.464 ± 0.003 ^b	69	31.7 ± 4.0	46	8.8883	—
K ₃ [Yb(CPAD) ₃]	DMSO	—	—	37.86 ± 0.06 ^c	—	1.12 ± 0.12	—	—	—
K[Eu(CPAP)(DMSO) ₂]	DMSO	25570 ± 350	20490 ± 270	1.702 ± 0.037 ^b	63	35.8 ± 3.7	57	9.2466	—
K[Yb(CPAP)(DMSO) ₂]	DMSO	—	—	8.91 ± 0.16 ^c	—	0.75 ± 0.02	—	—	—
K[Eu(CPAP)(H ₂ O) ₂]	water/DMSO ^d	—	—	0.382 ± 0.011 ^b	11	2.7 ± 0.4	25	—	1.9
K[Yb(CPAP)(H ₂ O) ₂]	water/DMSO ^d	—	—	0.52 ± 0.01 ^c	—	0.028 ± 0.002	—	—	—

^aObtained using the Gd^{III} complex at 77 K.⁶⁶ ^bIn milliseconds (ms). ^cIn microseconds (μ s). ^dTRIS/HCl buffered aqueous solution (pH ~ 7.4, 10% DMSO).

Table 2. Two-Photon Absorption Cross Sections (σ_{2PA}) of the Eu^{III} Complexes

complex	solvent	σ_{2PA} ^a [GM] ^b
K ₃ [Eu(CPAD) ₃]	DMSO	857 ± 24
K[Eu(CPAP)(DMSO) ₂]	DMSO	266 ± 34
K[Eu(CPAP)(H ₂ O) ₂]	water/DMSO ^c	228 ± 36

^a $\lambda_{exc} = 750$ nm. ^b1 GM = 10⁻⁵⁰ cm⁴ s photon⁻¹ molecule⁻¹. ^cTRIS/HCl buffered aqueous solution (pH ~ 7.4, 10% DMSO).

alter the population CT states.⁷¹ Thus, we prepared 0.2 mM solutions of K₃[Ln(CPAD)₃] (Ln = Eu^{III} or Yb^{III}) with varying amounts of methanol and glycerol to obtain a wide range of viscosities. This allowed us to observe changes in the emission intensity as a function of the viscosity using one- and two-photon excitation for the K₃[Eu(CPAD)₃] complex, the first example of viscosity sensing using Eu^{III}-centered emission in the visible region of the spectrum using two-photon excitation. Upon excitation through the ligand at 400 or 800 nm, the emission intensities increase by about 2-fold or 5.8-fold, respectively, as the viscosity increases (Figures 4(A) and 4(B)) in the range of 0–200 cP. This is in the same order of magnitude as the increase observed for the Yb^{III} complex described by Ning and co-workers for the same viscosity range.⁵⁹

Viscosity-dependent emission intensity is also observed for K₃[Yb(CPAD)₃] complex, as shown in Figure 5. An approximate 2-fold increase over the 0–200 cP range is seen, on the same order of magnitude of the only other example of Yb^{III}-centered emission used for viscosity sensing.⁵⁹

In addition to viscosity, the emission intensity can be influenced by the solvent oxygen content, as the interaction between oxygen and the triplet level of the ligand adds a nonradiative deactivation pathway that decreases the Eu^{III} emission lifetime.⁷² Methanol and glycerol have different amounts of dissolved oxygen; the mole fractions at 298 K and 101.3 kPa are 4.15 × 10⁻⁴ for methanol and 4.8 × 10⁻⁶–5.5 × 10⁻⁶ for glycerol.^{73,74} To ensure that emission behavior is due to solvent viscosity, and not quenching through oxygen,^{72,75} the emission lifetimes of the complexes were determined. At 1.318 ± 0.052 ms in methanol and at 1.298 ± 0.014 ms in 1:9 methanol/glycerol (Figures S26 and S27), these are equivalent. The emission intensity of both Eu^{III} and Yb^{III} complexes is independent of the amount of dissolved oxygen in solution as well (Figure S34). This confirms that there is no quenching, and thus the intensity changes are due to the viscosity of the medium. Another solvent property, namely its polarity, can influence the emission intensity of the Ln^{III} as well, as high polarity solvents can stabilize ligand CT states,⁴⁹ and thus the

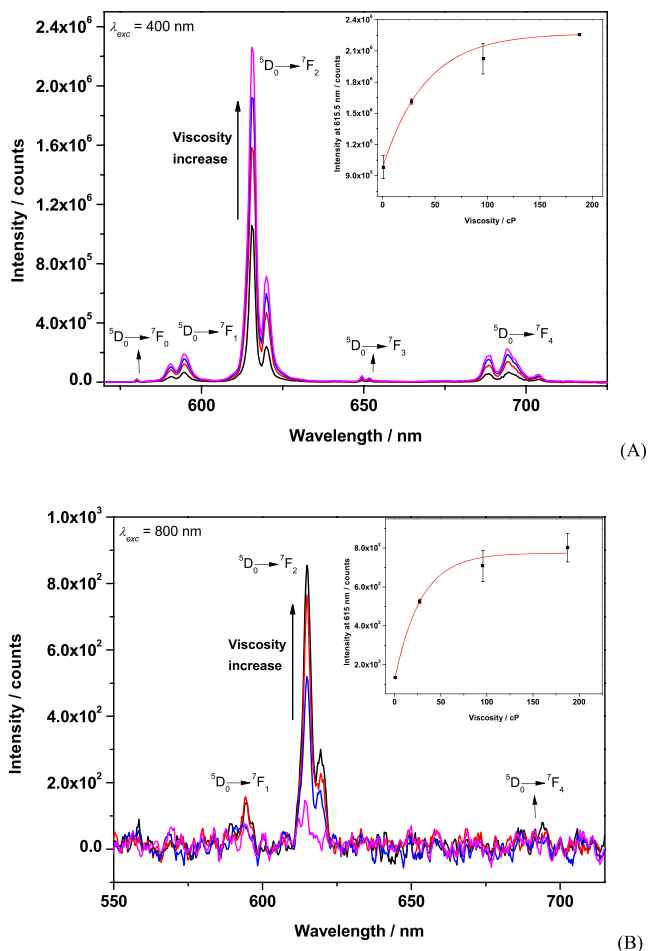


Figure 4. (A) Emission spectra of K₃[Eu(CPAD)₃] ($\lambda_{exc} = 400$ nm) upon one-photon excitation with varying viscosities. (B) Emission spectra of K₃[Eu(CPAD)₃] ($\lambda_{exc} = 720$ nm) upon two-photon excitation with varying viscosities. The insets show the plot of the emission intensity at 615.5 nm upon one-photon or two-photon excitation as a function of viscosity. [complex] = 1 × 10⁻⁴ M.

excited state energy of the ligand, which results in changes to the ligand → Ln^{III} energy transfer rates. To ensure that the energy of the ligand excited state is not affected by solvent polarity, the phosphorescence spectra of the [Gd(CPAD)₃] complex obtained in 100% methanol and mixture of methanol/glycerol (1:9) (Figure S35). The lack of significant change of the phosphorescence emission bands confirms that the polarity does not affect the energy levels of the ligand, and thus

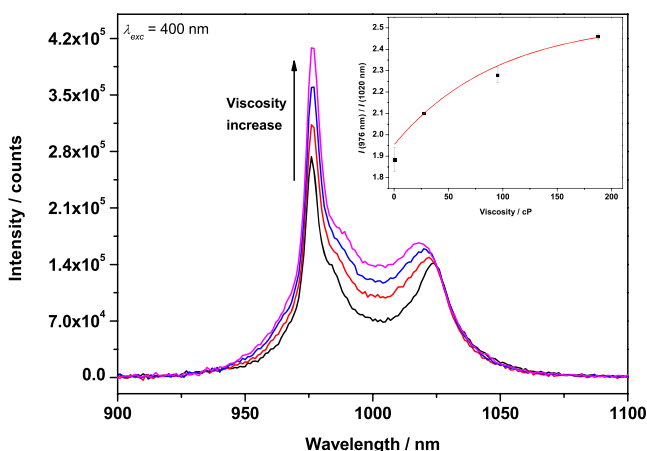


Figure 5. Emission spectra of $K_3[Yb(CPAD)_3]$ ($\lambda_{exc} = 400$ nm) upon one-photon excitation with varying viscosities. The inset shows the plot of the emission intensity ratios at 976 and 1020 nm upon one-photon excitation as a function of viscosity. Mixtures of MeOH/glycerol at various ratios were used as solvents with variable viscosity. $[complex] = 1 \times 10^{-4}$ M.

emission intensity changes are solely due to the viscosity of the medium.

CONCLUSIONS

A series of new Ln^{III} complexes containing new carbazole-based ligands were synthesized and their photophysical properties were measured. Eu^{III} emission efficiencies up to 35.8% were observed using one-photon excitation. Eu^{III} emission using 2PA was observed for all the complexes. The σ_{2PA} of 857 GM for $K_3[Eu(CPAD)_3]$ is, to date, the highest determined for Eu^{III} complexes in solution. A substantial change in emission intensity as a function of the viscosity was observed for $K_3[Eu(CPAD)_3]$ upon excitation with one-photon and, for the first time, two-photon excitation. Viscosity-dependent emission intensity is observed as well for the analogous Yb^{III} complex, which is only the second example of NIR Ln^{III} -based emission viscosity sensing. These complexes are thus effective sensors of the viscosity of the medium, which can be monitored through the intensity of the emitted light in the visible and NIR excited by either one or two photons. These results establish this carbazole-based family of ligands as a foundation for improved 2PA dyes and as viscosity sensors. This will contribute to the fields of imaging, sensing of physicochemical properties, and diagnosis in microscale systems.

EXPERIMENTAL SECTION

All commercially obtained reagents were of analytical grade and were used as received. Solvents were dried and purified by standard methods unless otherwise noted. All synthetic steps were completed under N_2 unless otherwise specified. The detailed synthetic procedures of the ligands and their Ln^{III} complexes are provided in the Supporting Information. Details of the one- and two-photon photophysical characterization and viscosity measurements are provided in the Supporting Information as well.

NMR Spectroscopy. All NMR spectra were recorded on Varian 400 and 500 MHz spectrometers with chemical shifts reported (δ , ppm) in deuterated chloroform ($CDCl_3$) against tetramethylsilane (TMS, 0.00 ppm) at 25.0 ± 0.1 °C.

Mass Spectrometry. Electrospray ionization mass spectra (ESI-MS) were collected in positive ion mode on a Waters Micromass ZQ quadrupole in the low-resolution mode for the ligands and on an

Agilent model G6230A with a QTOF analyzer in the high-resolution mode for the metal complexes. The samples were prepared by diluting acetonitrile solutions to a concentration of ~ 1 mg/mL and passing them through a 0.2 mm microfilter.

ASSOCIATED CONTENT

Supporting Information

The Supporting Information is available free of charge at <https://pubs.acs.org/doi/10.1021/acs.inorgchem.9b03561>.

Details of the synthesis and characterization, as well as spectra (PDF)

AUTHOR INFORMATION

Corresponding Author

Ana de Bettencourt-Dias – Department of Chemistry, University of Nevada, Reno, Nevada 89557, United States; orcid.org/0000-0001-5162-2393; Email: abd@unr.edu

Authors

Jorge H. S. K. Monteiro – Department of Chemistry, University of Nevada, Reno, Nevada 89557, United States

Natalie R. Fetto – Department of Chemistry, University of Nevada, Reno, Nevada 89557, United States

Matthew J. Tucker – Department of Chemistry, University of Nevada, Reno, Nevada 89557, United States; orcid.org/0000-0001-9724-4455

Complete contact information is available at:

<https://pubs.acs.org/doi/10.1021/acs.inorgchem.9b03561>

Author Contributions

The manuscript was written through contributions of all authors. All authors have given approval to the final version of the manuscript.

Notes

The authors declare no competing financial interest.

ACKNOWLEDGMENTS

The authors gratefully acknowledge the NSF and NIH for financial support of this work (CHE-1800392 to A.d.B.D. and R15GM1224597 to M.J.T., respectively).

REFERENCES

- Bünzli, J.-C. G. Lanthanide luminescence for biomedical analyses and imaging. *Chem. Rev.* **2010**, *110* (5), 2729–55.
- Zhao, J.; Gao, J.; Xue, W.; Di, Z.; Xing, H.; Lu, Y.; Li, L. Upconversion Luminescence-Activated DNA Nanodevice for ATP Sensing in Living Cells. *J. Am. Chem. Soc.* **2018**, *140* (2), 578–581.
- Hai, J.; Li, T.; Su, J.; Liu, W.; Ju, Y.; Wang, B.; Hou, Y. Anions Reversibly Responsive Luminescent Tb(III) Nanocellulose Complex Hydrogels for Latent Fingerprint Detection and Encryption. *Angew. Chem., Int. Ed.* **2018**, *57* (23), 6786–6790.
- Mathieu, E.; Sipo, A.; Demeyere, E.; Phipps, D.; Sakaveli, D.; Borbas, K. E. Lanthanide-based tools for the investigation of cellular environments. *Chem. Commun.* **2018**, *54*, 10021–10035.
- Kaczmarek, M. T.; Zabiszak, M.; Nowak, M.; Jastrzab, R. Lanthanides: Schiff base complexes, applications in cancer diagnosis, therapy, and antibacterial activity. *Coord. Chem. Rev.* **2018**, *370*, 42–54.
- Aulsebrook, M. L.; Graham, B.; Grace, M. R.; Tuck, K. L. Lanthanide complexes for luminescence-based sensing of low molecular weight analytes. *Coord. Chem. Rev.* **2018**, *375*, 191–220.
- Bünzli, J.-C. G. Luminescence bioimaging with lanthanide complexes. *Luminescence of Lanthanide Ions in Coordination Compounds and Nanomaterials* **2014**, 125–196.

- (8) Fordham, S.; Wang, X.; Bosch, M.; Zhou, H.-C. Lanthanide Metal-Organic Frameworks: Syntheses, Properties, and Potential Applications. *Struct. Bonding (Berlin, Ger.)* **2014**, *163*, 1–27.
- (9) Hewitt, S. H.; Butler, S. J. Application of lanthanide luminescence in probing enzyme activity. *Chem. Commun. (Cambridge, U. K.)* **2018**, *54* (50), 6635–6647.
- (10) Jia, J.-H.; Li, Q.-W.; Chen, Y.-C.; Liu, J.-L.; Tong, M.-L. Luminescent single-molecule magnets based on lanthanides: Design strategies, recent advances and magneto-luminescent studies. *Coord. Chem. Rev.* **2019**, *378*, 365–381.
- (11) Sy, M.; Nonat, A.; Hildebrandt, N.; Charbonniere, L. J. Lanthanide-based luminescence biolabelling. *Chem. Commun. (Cambridge, U. K.)* **2016**, *52* (29), 5080–5095.
- (12) Ning, Y.; Zhu, M.; Zhang, J.-L. Near-infrared (NIR) lanthanide molecular probes for bioimaging and biosensing. *Coord. Chem. Rev.* **2019**, *399*, 213028.
- (13) Ning, Y.; Cheng, S.; Wang, J.-X.; Liu, Y.-W.; Feng, W.; Li, F.; Zhang, J.-L. Fluorescence lifetime imaging of upper gastrointestinal pH in vivo with a lanthanide based near-infrared τ probe. *Chemical Science* **2019**, *10* (15), 4227–4235.
- (14) Ning, Y.; Tang, J.; Liu, Y.-W.; Jing, J.; Sun, Y.; Zhang, J.-L. Highly luminescent, biocompatible ytterbium(III) complexes as near-infrared fluorophores for living cell imaging. *Chem. Sci.* **2018**, *9* (15), 3742–3753.
- (15) Ning, Y.; Ke, X.-S.; Hu, J.-Y.; Liu, Y.-W.; Ma, F.; Sun, H.-L.; Zhang, J.-L. Bioinspired Orientation of β -Substituents on Porphyrin Antenna Ligands Switches Ytterbium(III) NIR Emission with Thermosensitivity. *Inorg. Chem.* **2017**, *56* (4), 1897–1905.
- (16) Bünzli, J.-C. G. On the design of highly luminescent lanthanide complexes. *Coord. Chem. Rev.* **2015**, *293–294* (0), 19–47.
- (17) de Bettencourt-Dias, A. Introduction to Lanthanide Ion Luminescence. *Luminescence of Lanthanide Ions in Coordination Compounds and Nanomaterials* **2014**, *1*.
- (18) Bünzli, J.-C. G.; Piguet, C. Taking advantage of luminescent lanthanide ions. *Chem. Soc. Rev.* **2005**, *34* (12), 1048–1077.
- (19) Monteiro, J.; Machado, D.; de Hollanda, L. M.; Lancellotti, M.; Sigoli, F. A.; de Bettencourt-Dias, A. Selective cytotoxicity and luminescence imaging of cancer cells with a dipicolinato-based Eu-III complex. *Chem. Commun.* **2017**, *53* (86), 11818–11821.
- (20) Law, G. L.; Pal, R.; Palsson, L. O.; Parker, D.; Wong, K. L. Responsive and reactive terbium complexes with an azaxanthone sensitizer and one naphthyl group: applications in ratiometric oxygen sensing in vitro and in regioselective cell killing. *Chem. Commun. (Cambridge, U. K.)* **2009**, *0* (47), 7321–3.
- (21) Ren, T.; Xu, W.; Zhang, Q.; Zhang, X.; Wen, S.; Yi, H.; Yuan, L.; Zhang, X. Harvesting Hydrogen Bond Network: Enhance the Anti-Solvatochromic Two-Photon Fluorescence for Cirrhosis Imaging. *Angew. Chem., Int. Ed.* **2018**, *57* (25), 7473–7477.
- (22) Agrawalla, B. K.; Lee, H. W.; Phue, W. H.; Raju, A.; Kim, J. J.; Kim, H. M.; Kang, N. Y.; Chang, Y. T. Two-Photon Dye Cocktail for Dual-Color 3D Imaging of Pancreatic Beta and Alpha Cells in Live Islets. *J. Am. Chem. Soc.* **2017**, *139* (9), 3480–3487.
- (23) Agrawalla, B. K.; Chandran, Y.; Phue, W. H.; Lee, S. C.; Jeong, Y. M.; Wan, S. Y. D.; Kang, N. Y.; Chang, Y. T. Glucagon-Secreting Alpha Cell Selective Two-Photon Fluorescent Probe TP-alpha: For Live Pancreatic Islet Imaging. *J. Am. Chem. Soc.* **2015**, *137* (16), 5355–5362.
- (24) Kumari, P.; Verma, S. K.; Mobin, S. M. Water soluble two-photon fluorescent organic probes for long-term imaging of lysosomes in live cells and tumor spheroids. *Chem. Commun.* **2018**, *54* (5), 539–542.
- (25) Bünzli, J.-C. G.; Eliseeva, S. V. Basics of Lanthanide Photophysics. *Springer Ser. Fluoresc.* **2010**, *7*, 1–45.
- (26) Denk, W.; Strickler, J. H.; Webb, W. W. 2-Photon laser scanning fluorescence microscopy. *Science* **1990**, *248* (4951), 73–76.
- (27) Helmchen, F.; Denk, W. Deep tissue two-photon microscopy. *Nat. Methods* **2005**, *2* (12), 932–940.
- (28) Liu, B.; Li, C.; Yang, P.; Hou, Z.; Lin, J. 808-nm-Light-Excited Lanthanide-Doped Nanoparticles: Rational Design, Luminescence Control and Theranostic Applications. *Adv. Mater. (Weinheim, Ger.)* **2017**, *29* (18), 1605434.
- (29) Nguyen, T. N.; Ebrahim, F. M.; Stylianou, K. C. Photoluminescent, upconversion luminescent and nonlinear optical metal-organic frameworks: From fundamental photophysics to potential applications. *Coord. Chem. Rev.* **2018**, *377*, 259–306.
- (30) Terenziani, F.; Katan, C.; Badaeva, E.; Tretiak, S.; Blanchard-Desce, M. Enhanced Two-Photon Absorption of Organic Chromophores: Theoretical and Experimental Assessments. *Adv. Mater.* **2008**, *20* (24), 4641–4678.
- (31) Andraud, C.; Maury, O. Lanthanide Complexes for Nonlinear Optics: From Fundamental Aspects to Applications. *Eur. J. Inorg. Chem.* **2009**, *2009* (29–30), 4357–4371.
- (32) Li, B.; Lu, L.; Zhao, M.; Lei, Z.; Zhang, F. An Efficient 1064 nm NIR-II Excitation Fluorescent Molecular Dye for Deep-Tissue High-Resolution Dynamic Bioimaging. *Angew. Chem., Int. Ed.* **2018**, *57* (25), 7483–7487.
- (33) Nam, J. S.; Kang, M. G.; Kang, J.; Park, S. Y.; Lee, S. J. C.; Kim, H. T.; Seo, J. K.; Kwon, O. H.; Lim, M. H.; Rhee, H. W.; Kwon, T. H. Endoplasmic Reticulum-Localized Iridium(III) Complexes as Efficient Photodynamic Therapy Agents via Protein Modifications. *J. Am. Chem. Soc.* **2016**, *138* (34), 10968–10977.
- (34) Tian, R.; Sun, W.; Li, M.; Long, S.; Li, M.; Fan, J.; Guo, L.; Peng, X. Development of an anti-tumor theranostic platform: a near-infrared molecular upconversion sensitizer for deep-seated cancer photodynamic therapy. *Chemical Science* **2019**, *10*, 10106–10112.
- (35) Lakowicz, J. R.; Piszczek, G.; P. Maliwal, B.; Gryczynski, I. Multiphoton excitation of lanthanides. *ChemPhysChem* **2001**, *2* (4), 247–252.
- (36) Piszczek, G.; Maliwal, B. P.; Gryczynski, I.; Dattelbaum, J.; Lakowicz, J. R. Multiphoton ligand-enhanced excitation of lanthanides. *J. Fluoresc.* **2001**, *11* (2), 101–107.
- (37) Picot, A.; D'Aleo, A.; Baldeck, P. L.; Grichine, A.; Duperray, A.; Andraud, C.; Maury, O. Long-lived two-photon excited luminescence of water-soluble europium complex: Applications in biological imaging using two-photon scanning microscopy. *J. Am. Chem. Soc.* **2008**, *130* (5), 1532–1533.
- (38) Grichine, A.; Haeefe, A.; Pascal, S.; Duperray, A.; Michel, R.; Andraud, C.; Maury, O. Millisecond lifetime imaging with a europium complex using a commercial confocal microscope under one or two-photon excitation. *Chemical Science* **2014**, *5* (9), 3475–3485.
- (39) Bui, A. T.; Grichine, A.; Bresselet, S.; Duperray, A.; Andraud, C.; Maury, O. Unexpected Efficiency of a Luminescent Samarium(III) Complex for Combined Visible and Near-Infrared Biphotonic Microscopy. *Chem. - Eur. J.* **2015**, *21* (49), 17757–17761.
- (40) Law, G. L.; Wong, K. L.; Man, C. W. Y.; Tsao, S. W.; Wong, W. T. A two-photon europium complex as specific endoplasmic reticulum probe. *J. Biophotonics* **2009**, *2* (12), 718–724.
- (41) Placide, V.; Bui, A. T.; Grichine, A.; Duperray, A.; Pitrat, D.; Andraud, C.; Maury, O. Two-photon multiplexing bio-imaging using a combination of Eu- and Tb-bioprobes. *Dalton Trans.* **2015**, *44* (11), 4918–4924.
- (42) Bui, A. T.; Beyler, M.; Liao, Y. Y.; Grichine, A.; Duperray, A.; Mulatier, J. C.; Le Guennic, B.; Andraud, C.; Maury, O.; Tripier, R. Cationic Two-Photon Lanthanide Bioprobes Able to Accumulate in Live Cells. *Inorg. Chem.* **2016**, *55* (14), 7020–7025.
- (43) Palsson, L. O.; Pal, R.; Murray, B. S.; Parker, D.; Beeby, A. Two-photon absorption and photoluminescence of europium based emissive probes for bioactive systems. *Dalton Trans.* **2007**, *0* (48), 5726–5734.
- (44) D'Aléo, A.; Pointillart, F.; Ouahab, L.; Andraud, C.; Maury, O. Charge transfer excited states sensitization of lanthanide emitting from the visible to the near-infra-red. *Coord. Chem. Rev.* **2012**, *256* (15–16), 1604–1620.
- (45) D'Aleo, A.; Picot, A.; Baldeck, P. L.; Andraud, C.; Maury, O. Design of Dipicolinic Acid Ligands for the Two-Photon Sensitized Luminescence of Europium Complexes with Optimized Cross-Sections. *Inorg. Chem.* **2008**, *47* (22), 10269–10279.

- (46) Picot, A.; Malvolti, F.; Le Guennic, B.; Baldeck, P. L.; Williams, J. A. G.; Andraud, C.; Maury, O. Two-photon antenna effect induced in octupolar europium complexes. *Inorg. Chem.* **2007**, *46* (7), 2659–2665.
- (47) Eliseeva, S. V.; Auböck, G.; van Mourik, F.; Cannizzo, A.; Song, B.; Deiters, E.; Chauvin, A.-S.; Chergui, M.; Bünzli, J.-C. G. Multiphoton-Excited Luminescent Lanthanide Bioprobes: Two- and Three-Photon Cross Sections of Dipicolinate Derivatives and Binuclear Helicates. *J. Phys. Chem. B* **2010**, *114*, 2932–2937.
- (48) D'Aléo, A.; Pompidor, G.; Elena, B.; Vicat, J.; Baldeck, P. L.; Toupet, L.; Kahn, R.; Andraud, C.; Maury, O. Two-photon microscopy and spectroscopy of lanthanide bio-probes. *ChemPhysChem* **2007**, *8* (14), 2125–2132.
- (49) Andraud, C.; Maury, O. Lanthanide Complexes for Nonlinear Optics: From Fundamental Aspects to Applications. *Eur. J. Inorg. Chem.* **2009**, 2009 (29–30), 4357–4371.
- (50) D'Aléo, A.; Andraud, C.; Maury, O. Two-photon Absorption of Lanthanide Complexes: from Fundamental Aspects to Biphonic Imaging Applications. *Luminescence of Lanthanide Ions in Coordination Compounds and Nanomaterials* **2014**, 197–230.
- (51) D'Aléo, A.; Picot, A.; Baldeck, P. L.; Andraud, C.; Maury, O. Design of Dipicolinic Acid Ligands for the Two-Photon Sensitized Luminescence of Europium Complexes with Optimized Cross-Sections. *Inorg. Chem.* **2008**, *47* (22), 10269–10279.
- (52) Yang, Z.; Cao, J.; He, Y.; Yang, J. H.; Kim, T.; Peng, X.; Kim, J. S. Macro-/micro-environment-sensitive chemosensing and biological imaging. *Chem. Soc. Rev.* **2014**, *43* (13), 4563–4601.
- (53) Kuimova, M. K.; Botchway, S. W.; Parker, A. W.; Balaz, M.; Collins, H. A.; Anderson, H. L.; Suhling, K.; Ogilby, P. R. Imaging intracellular viscosity of a single cell during photoinduced cell death. *Nat. Chem.* **2009**, *1* (1), 69–73.
- (54) Kuimova, M. K. Mapping viscosity in cells using molecular rotors. *Phys. Chem. Chem. Phys.* **2012**, *14* (37), 12671–12686.
- (55) Sloop, G.; Holsworth, R. E.; Weidman, J. J.; St Cyr, J. A. The role of chronic hyperviscosity in vascular disease. *Ther. Adv. Cardiovasc. Dis.* **2015**, *9* (1), 19–25.
- (56) Haidekker, M. A.; Brady, T. P.; Lichlyter, D.; Theodorakis, E. A. A ratiometric fluorescent viscosity sensor. *J. Am. Chem. Soc.* **2006**, *128* (2), 398–399.
- (57) Kuimova, M. K.; Yahioglu, G.; Levitt, J. A.; Suhling, K. Molecular rotor measures viscosity of live cells via fluorescence lifetime imaging. *J. Am. Chem. Soc.* **2008**, *130* (21), 6672–6673.
- (58) Lee, S.-C.; Heo, J.; Woo, H. C.; Lee, J.-A.; Seo, Y. H.; Lee, C.-L.; Kim, S.; Kwon, O.-P. Fluorescent Molecular Rotors for Viscosity Sensors. *Chem. - Eur. J.* **2018**, *24*, 13706–13718.
- (59) Ning, Y.; Liu, Y.-W.; Meng, Y.-S.; Zhang, J.-L. Design of Near-Infrared Luminescent Lanthanide Complexes Sensitive to Environmental Stimulus through Rationally Tuning the Secondary Coordination Sphere. *Inorg. Chem.* **2018**, *57* (3), 1332–1341.
- (60) Bui, A. T.; Grichine, A.; Duperray, A.; Lidon, P.; Riobe, F.; Andraud, C.; Maury, O. Terbium(III) Luminescent Complexes as Millisecond-Scale Viscosity Probes for Lifetime Imaging. *J. Am. Chem. Soc.* **2017**, *139* (23), 7693–7696.
- (61) Monteiro, J. H. S. K.; de Bettencourt-Dias, A.; Sigoli, F. A. Estimating the Donor–Acceptor Distance To Tune the Emission Efficiency of Luminescent Lanthanide Compounds. *Inorg. Chem.* **2017**, *56* (2), 709–712.
- (62) Monteiro, J. H. S. K.; Sigoli, F. A.; de Bettencourt-Dias, A. A Water-soluble Tb^{III} complex as temperature-sensitive luminescent probe. *Can. J. Chem.* **2018**, *96* (9), 859–864.
- (63) Lepeltier, M.; Appaix, F.; Liao, Y. Y.; Dumur, F.; Marrot, J.; Le Bahers, T.; Andraud, C.; Monnereau, C. Carbazole-Substituted Iridium Complex as a Solid State Emitter for Two-Photon Intravital Imaging. *Inorg. Chem.* **2016**, *55* (19), 9586–9595.
- (64) Hao, X. L.; Zhang, L.; Wang, D.; Zhang, C.; Guo, J. F.; Ren, A. M. Analyzing the Effect of Substituents on the Photophysical Properties of Carbazole-Based Two-Photon Fluorescent Probes for Hypochlorite in Mitochondria. *J. Phys. Chem. C* **2018**, *122* (11), 6273–6287.
- (65) Chen, P. Z.; Wang, J. X.; Niu, L. Y.; Chen, Y. Z.; Yang, Q. Z. Carbazole-containing difluoroboron beta-diketonate dyes: two-photon excited fluorescence in solution and grinding-induced blue-shifted emission in the solid state. *J. Mater. Chem. C* **2017**, *5* (47), 12538–12546.
- (66) Crosby, G. A.; Whan, R. E.; Alire, R. M. Intramolecular Energy Transfer in Rare Earth Chelates. Role of the Triplet State. *J. Chem. Phys.* **1961**, *34* (3), 743–748.
- (67) Caillé, F.; Bonnet, C. S.; Buron, F.; Villette, S.; Helm, L.; Petoud, S.; Suzenet, F.; Tóth, É. Isoquinoline-Based Lanthanide Complexes: Bright NIR Optical Probes and Efficient MRI Agents. *Inorg. Chem.* **2012**, *51* (4), 2522–2532.
- (68) de Bettencourt-Dias, A.; Barber, P. S.; Viswanathan, S.; de Lill, D. T.; Rollett, A.; Ling, G.; Altun, S. Para-derivatized pybox ligands as sensitizers in highly luminescent Ln(III) complexes. *Inorg. Chem.* **2010**, *49* (19), 8848–61.
- (69) Makarov, N. S.; Drobizhev, M.; Rebane, A. Two-photon absorption standards in the 550–1600 nm excitation wavelength range. *Opt. Express* **2008**, *16* (6), 4029–4047.
- (70) Kato, S.; Matsumoto, T.; Shigeiwa, M.; Gorohmaru, H.; Maeda, S.; Ishi-i, T.; Mataka, S. Novel 2,1,3-benzothiadiazole-based red-fluorescent dyes with enhanced two-photon absorption cross-sections. *Chem. - Eur. J.* **2006**, *12* (8), 2303–2317.
- (71) Sasaki, S.; Drummen, G. P. C.; Konishi, G. Recent advances in twisted intramolecular charge transfer (TICT) fluorescence and related phenomena in materials chemistry. *J. Mater. Chem. C* **2016**, *4* (14), 2731–2743.
- (72) Walter, E. R. H.; Williams, J. A. G.; Parker, D. Solvent polarity and oxygen sensitivity, rather than viscosity, determine lifetimes of biaryl-sensitized terbium luminescence. *Chem. Commun.* **2017**, *53*, 13344–13347.
- (73) Kutsche, I.; Gildehaus, G.; Schuller, D.; Schumpe, A. Oxygen Solubilities in Aqueous Alcohol Solutions. *J. Chem. Eng. Data* **1984**, *29*, 286–287.
- (74) Sato, T.; Hamada, Y.; Sumikawa, M.; Araki, S.; Yamamoto, H. Solubility of Oxygen in Organic Solvents and Calculation of the Hansen Solubility Parameters of Oxygen. *Ind. Eng. Chem. Res.* **2014**, *53*, 19331–19337.
- (75) Bui, A. T.; Grichine, A.; Duperray, A.; Lidon, P.; Riobé, F.; Andraud, C.; Maury, O. Terbium(III) Luminescent Complexes as Millisecond-Scale Viscosity Probes for Lifetime Imaging. *J. Am. Chem. Soc.* **2017**, *139*, 7693–7696.